

Direct photons in high energy proton-proton and nucleus-nucleus collisions

Sushobhan Kumar Mandal

National Center for Nuclear Research
Warsaw, Poland

June 1, 2023

① Theoretical introduction

- Quark-gluon plasma
- Heavy ion collisions
- Direct photons and their sources

② Experimental situations

- How we measure direct photons
- Data from WA98
- Data from RHIC
- Data from LHC

③ My work so far

- Quality assurance
- Energy calibration

④ Upcoming work plan

⑤ Summary

Theoretical introduction

Standard model and strong interaction

QUARKS

UP mass 2,3 MeV/c ² charge 2/3 spin 1/2 	CHARM 1,275 GeV/c ² 2/3 1/2 	TOP 173,07 GeV/c ² 2/3 1/2 	GLUON 0 0 1 	HIGGS BOSON 126 GeV/c ² 0 0
DOWN 4,8 MeV/c ² -1/3 1/2 	STRANGE 95 MeV/c ² -1/3 1/2 	BOTTOM 4,18 GeV/c ² -1/3 1/2 	PHOTON 0 0 1 	

LEPTONS

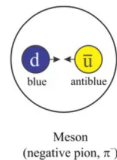
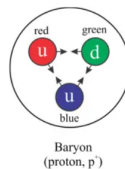
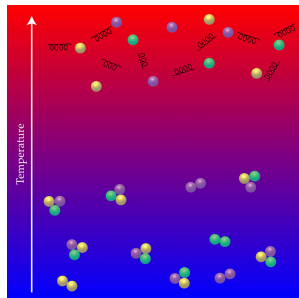
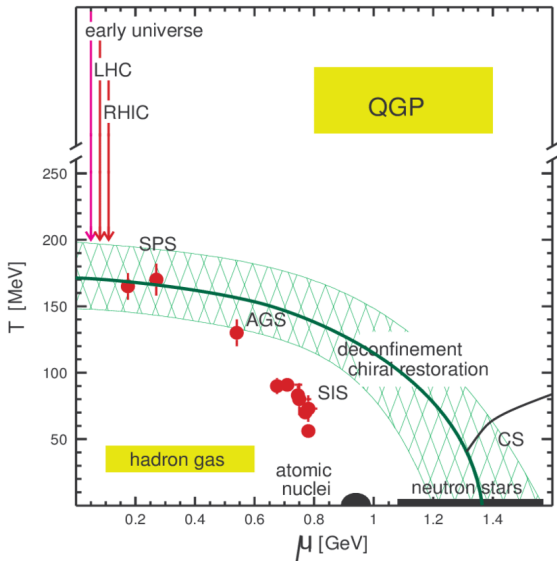
ELECTRON 0,511 MeV/c ² -1 1/2 	MUON 105,7 MeV/c ² -1 1/2 	TAU 1,777 GeV/c ² -1 1/2
ELECTRON NEUTRINO <2,2 eV/c ² 0 1/2 	MUON NEUTRINO <0,17 MeV/c ² 0 1/2 	TAU NEUTRINO <15,5 MeV/c ² 0 1/2

GAUGE BOSONS

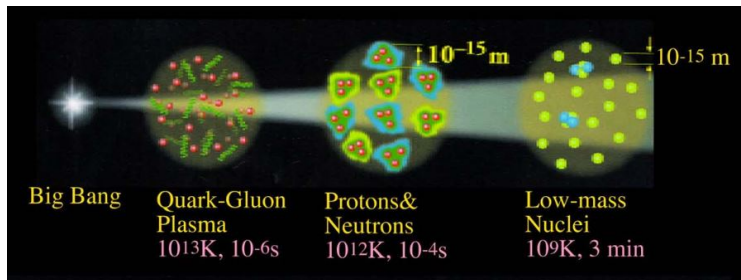
Z BOSON 91,2 GeV/c ² 0 -1 1
W BOSON 80,4 GeV/c ² ±1 1

- Quarks and Gluons carry three types of color charges
- Gluons act as mediators between the quarks resulting strong interaction
- Gluons also take part in strong interaction
- Bound states of quarks are formed resulting ordinary matter around us

Phase transition in QCD



Early universe and Quark deconfinement



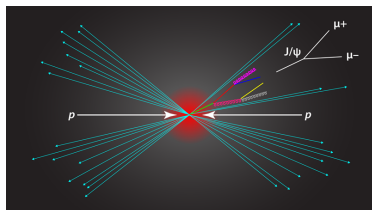
- After big bang (few microseconds old) universe is believed to be filled with deconfined state of quarks and gluons.
- Heavy-ion collisions recreate in the labs, such droplets of matter that filled the universe about 1 microsecond after the big bang
- With heavy-ion collisions we can learn about the properties (Not possible with astronomical) at very temperature and density and explore QCD phase diagram

Differences between p-p Collisions and A-A Collisions in QGP Study

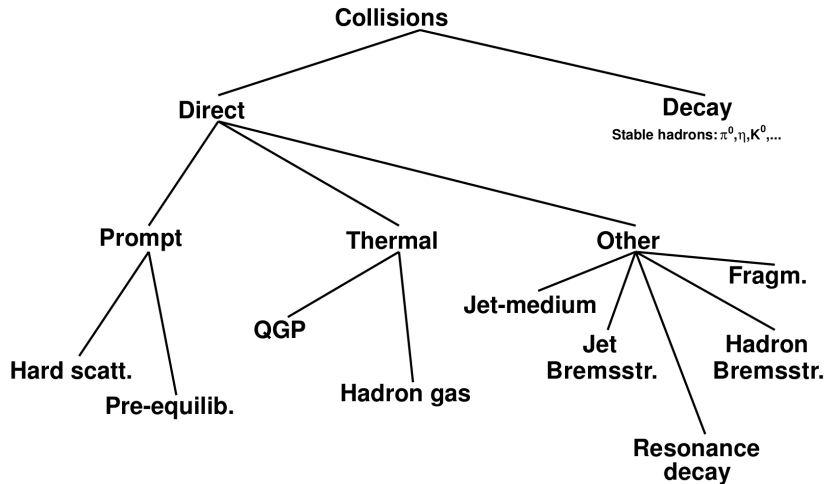
- Energy density:
 - p-p collisions: Typically a few GeV/fm^3
 - A-A collisions: $10\text{-}20 \text{ GeV}/\text{fm}^3$ or higher
- Temperature:
 - A-A collisions: Several hundred MeV to over a trillion degrees Kelvin
- Size and lifetime of the QGP:
 - p-p collisions: Highly transient and smaller in size
 - A-A collisions: Spatial extent of several femtometers, lasting tens to hundreds of femtoseconds
- Particle multiplicity:
 - A-A collisions: Significantly larger number of particles compared to p-p collisions
- Jet quenching:
 - A-A collisions: Much more pronounced, resulting in stronger energy loss and modification of jet-related observables

Different ways to study QGP

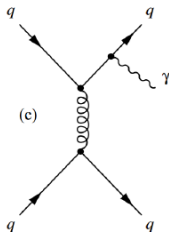
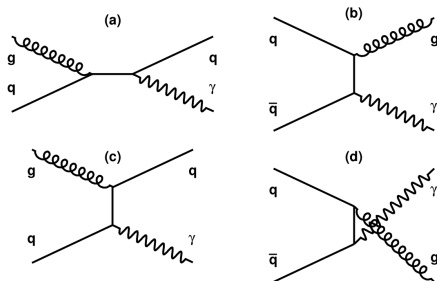
- $J/\psi(c\bar{c})$ suppression
 - Jet quenching
 - Direct Photons
- etc.



Photons in heavy ion collisions



Feynman diagrams contributing to Direct Photon production



Experimental situation

Techniques for Photon Detection

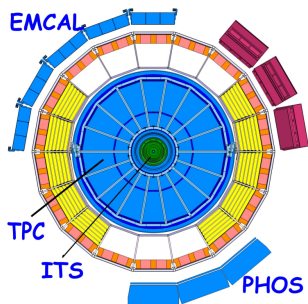


Figure: Photon detection methods at ALICE, LHC

- Photon conversion method:
 - Utilizes the conversion of photons into electron-positron pairs in a detector material
 - Tracks of the converted electrons and positrons are measured to reconstruct the original photon properties
- Calorimetry:
 - Measures the energy of particles by absorbing them in a material and detecting the resulting electromagnetic shower
 - Photon-induced showers are identified and their energy is measured in the calorimeter
 - Provides good energy resolution and allows for the study of high-energy photons in the QGP

Procedure for Direct Photon Measurements

Hadron	Decay
π^0	$\gamma\gamma$
η	$\gamma\gamma$
ω	$\pi^0\gamma$
η'	$\rho\gamma$
ϕ	$\eta\gamma$
ρ^0	$\pi^+\pi^-\gamma$

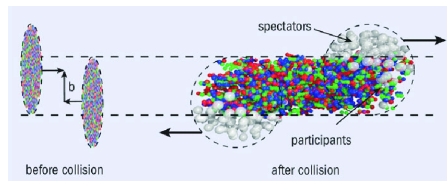
Table: Hadronic decay to photons

- Measurement of inclusive photon spectra
- Determination of decay photon spectra through Monte Carlo simulation as well as neutral meson measurement
- Subtract decay photon yield (γ_{decay}) from inclusive photon yield (γ_{incl})

$$\gamma_{direct} = \gamma_{incl} - \gamma_{decay} = \left(1 - \frac{1}{R_\gamma}\right) \cdot \gamma_{incl}$$

Figure: Direct photon yield

Collision centrality in heavy ion collision



Collision centrality	Centrality bin number
0-20%	0
20-40%	1
40-60%	2
60-80%	3
80-100%	4

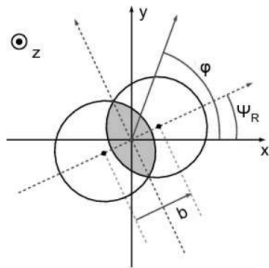
Table: Collision centrality and centrality bins

$$\text{Centrality} = \frac{\text{spectator}}{\text{All}}$$

Anisotropic Collective Flow

The initial spatial anisotropy of non-central ion-ion collision leads to the build-up of collective anisotropic flow, which is described in the distribution of final state particles as a function of azimuthal angle φ :

$$\frac{dN}{d\varphi} = \frac{N}{2\pi} \cdot \left(1 + \sum_{n>1} v_n \cos(n[\varphi - \Psi_R]) \right), \quad (6)$$



Analysis results from previous experiments

WA98 (West Area experiment)

Super Proton Synchrotron (SPS)

CERN

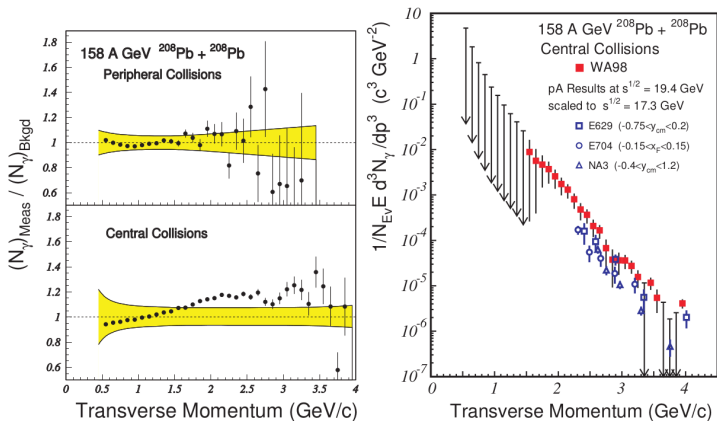
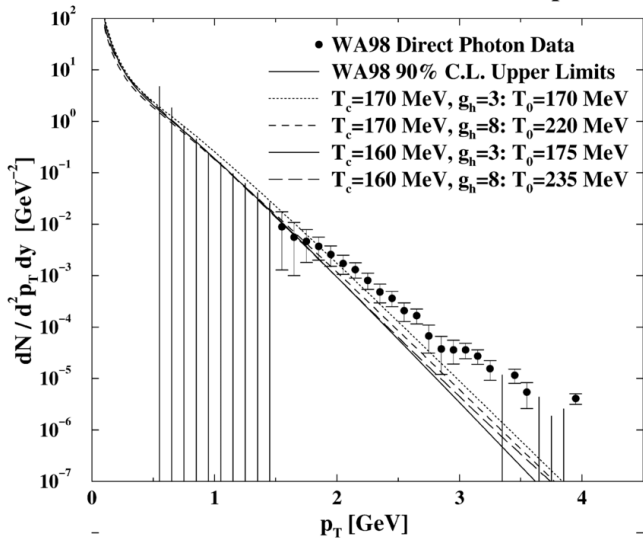


FIG. 18. Direct photon result from the WA98 experiment, 158 A GeV $^{208}\text{Pb} + ^{208}\text{Pb}$ collisions [70]. (Left panel) The ratio of measured inclusive photons to calculated decay photons as a function of p_T for peripheral (a) and central (b) collisions. Error bars on the data are statistical only, the p_T -dependent systematic uncertainties are shown as shaded bands. (Right panel) The invariant direct photon yield for central collisions. Error bars indicate combined statistical and systematic uncertainties. Data points with downward arrows indicate 90% C.L. upper limits ($\gamma_{\text{excess}} + 1.28\sigma_{\text{upper}}$). The data are compared to expected, N_{coll} -scaled pp yields from three earlier experiments (see explanation in the text). (Figures taken from [70].)

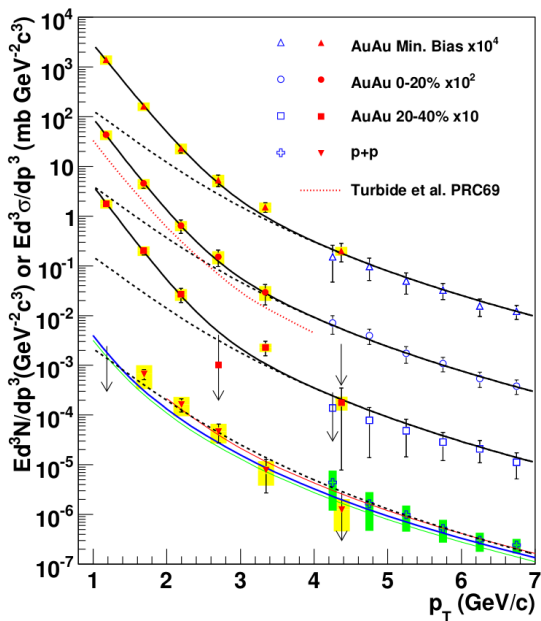
WA98 Direct Photon Data & Thermal Spectrum



PHENIX

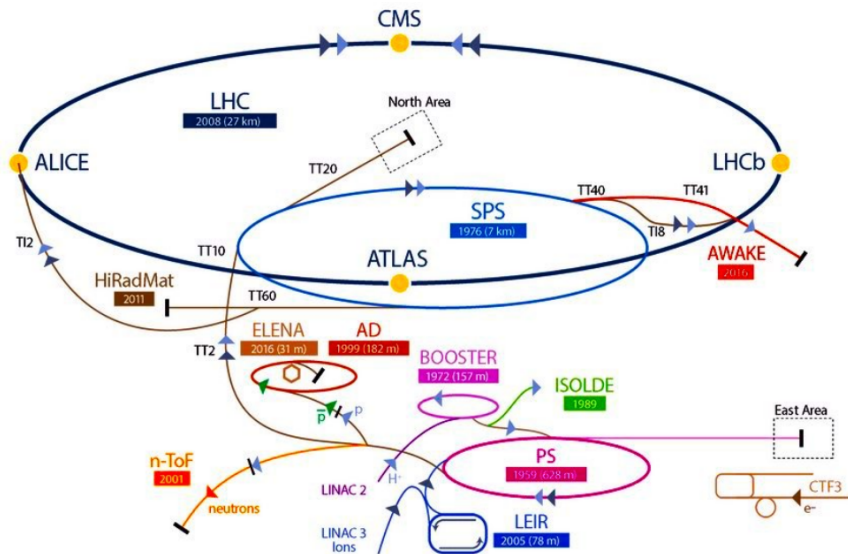
(Pioneering High Energy Nuclear Interaction eXperiment)

Relativistic Heavy Ion Collider (RHIC)
Brookhaven National Laboratory, United States



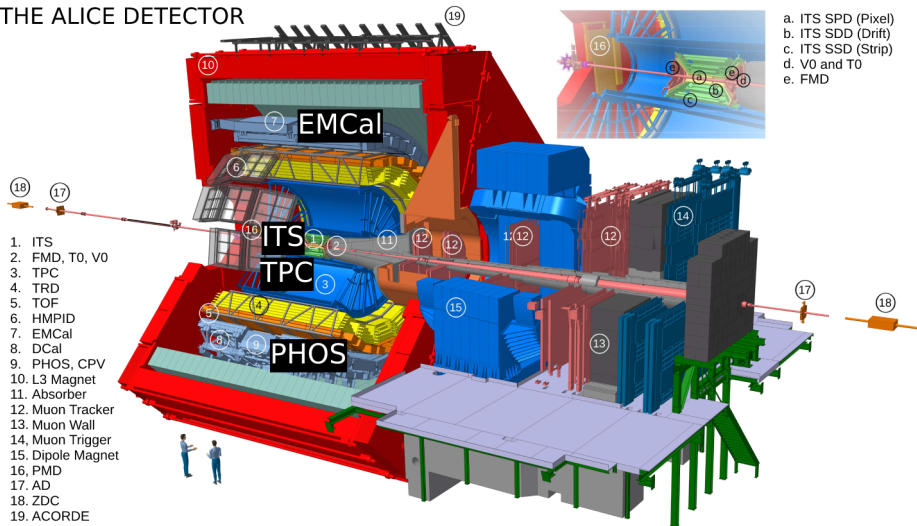
LHC and ALICE experiment

LHC schematics during Run2



A Large Ion Collider Experiment (ALICE schematic during Run2)

THE ALICE DETECTOR



ALICE and PHOton Spectrometer(PHOS)

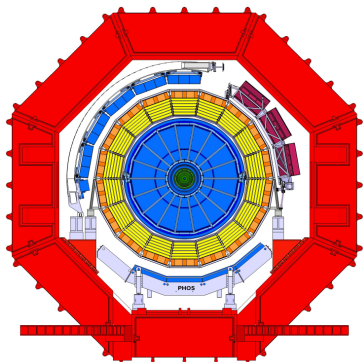


Figure: ALICE cross-sectional view in Run 2

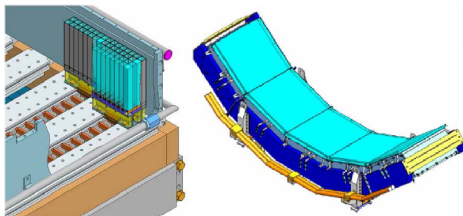


Figure: PHOS modules and its crystals



Figure: A detector element consisting PbWO₄ crystal, APD(Avalanche Photo Diode) detector and preamplifier

Coverage in pseudo-rapidity	$-0.125 \leq \eta \leq 0.125$
Coverage in azimuthal angle	$\Delta\varphi = 70^\circ$
Distance to interaction point	460 cm
Modularity	Three modules with 3584 and one with 1792 crystals
Material	Lead-tungstate (PbWO ₄) crystals
Crystal dimensions	$22 \times 22 \times 180 \text{ mm}^3$
Depth in radiation length	$20 X_0$
Number of crystals	12 544
Total area	6.0 m^2
Operating temperature	-25° C

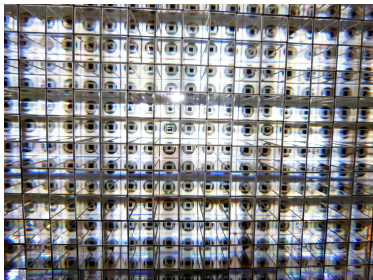


Figure: Part of cell matrix of one module

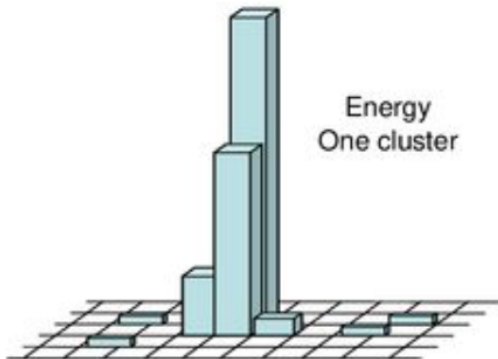


Figure: Cluster created by photon in PHOS cells.

Vertical column represents the amount of energy(not scaled) deposited in a PHOS cell

- With PHOS granularity, the energy deposited in the central cell is around 80% of the total cluster energy

Results from ALICE experiment :

$$\sqrt{S_{NN}} = 2.76 \text{ TeV}$$

$$R_\gamma \equiv \frac{\gamma_{\text{incl}}}{\pi_{\text{param}}^0} \bigg/ \frac{\gamma_{\text{decay}}}{\pi_{\text{param}}^0} = \frac{\gamma_{\text{incl}}}{\gamma_{\text{decay}}},$$

$$\gamma_{\text{direct}} = \gamma_{\text{incl}} - \gamma_{\text{decay}} = \left(1 - \frac{1}{R_\gamma}\right) \cdot \gamma_{\text{incl}}.$$

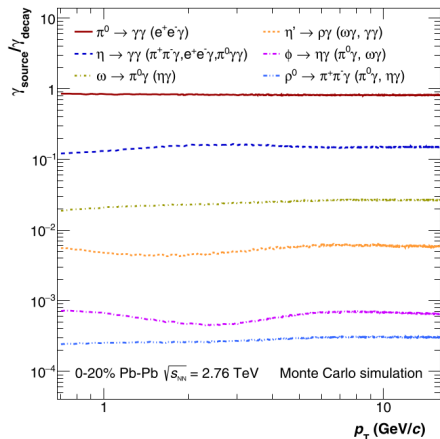
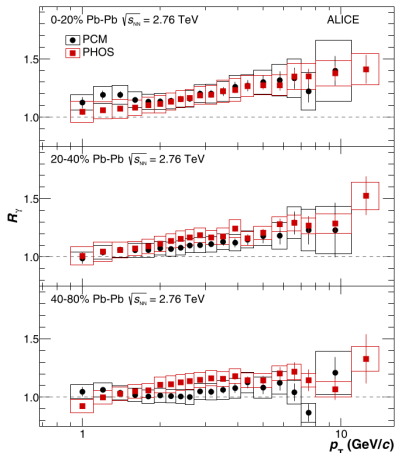
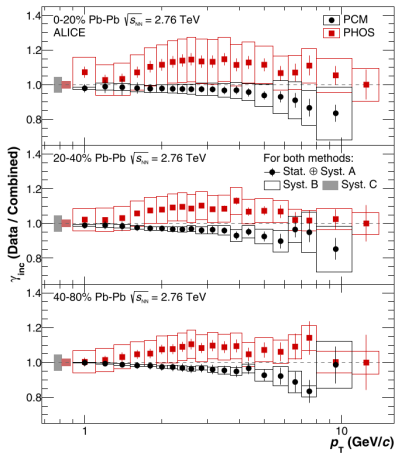
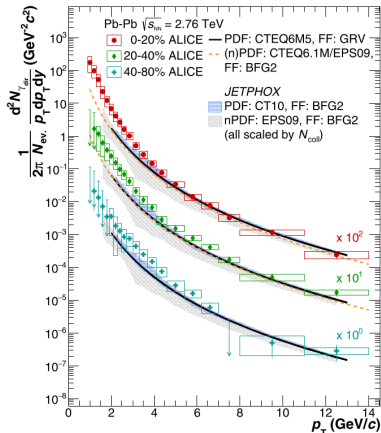
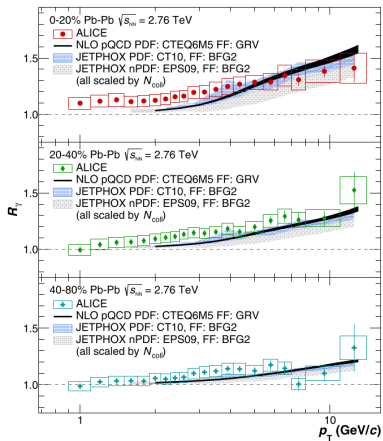


Fig. 1. (Color online.) Relative contributions of different hadrons to the total decay photon spectrum as a function of the decay photon transverse momentum (PCM case).

Inclusive and Direct Photons



Direct Photons



Results from PHENIX and ALICE

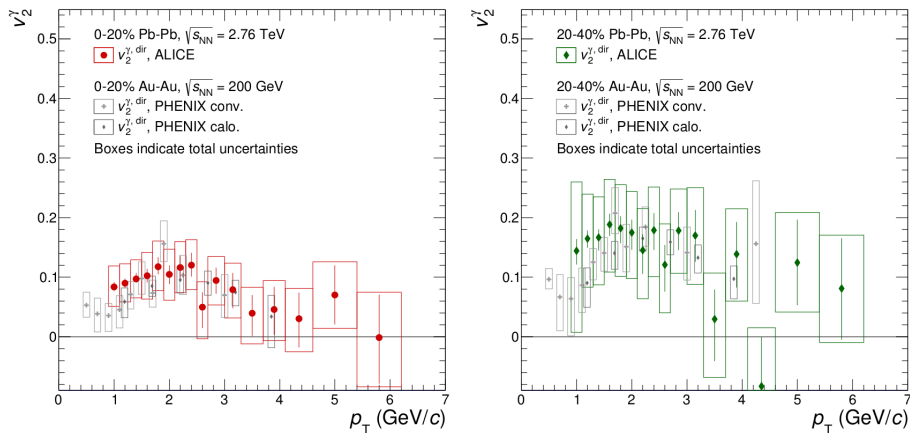
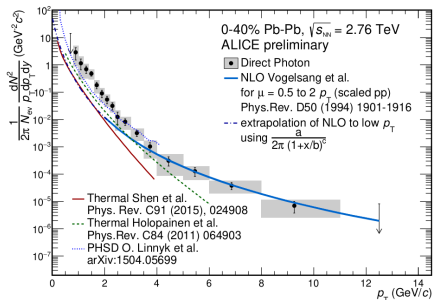


Fig. 5: (Color online) Elliptic flow of direct photons compared with PHENIX results [26] for the 0–20% (left) and 20–40% (right) centrality classes. The vertical bars on each data point indicate the statistical uncertainties and the boxes the total uncertainty.

Temperature estimation



$$A \cdot \exp\left(-\frac{p_T}{T_{\text{eff}}}\right) \text{ for } p_T \leq 2.2 \text{ GeV}/c$$

$$T_{\text{eff}} = 304 \pm 51_{\text{stat+sys}} \text{ MeV (ALICE, LHC)}$$

$$T_{\text{eff}} = 219 \pm 19_{\text{stat}} \pm 19_{\text{sys}} \text{ MeV (PHENIX, RHIC)}$$

Advantages of Higher Energy (5.02 TeV)

- Increased energy density of the QGP:
 - Higher collision energy leads to a higher initial energy density of the created QGP. This allows for the formation of a more strongly interacting and longer-lived QGP state.
 - The higher energy density enables the exploration of the QGP phase diagram in more extreme conditions, providing insights into the behavior of matter under more extreme temperatures and densities.
- Enhanced temperature of the QGP:
 - The higher collision energy corresponds to a higher temperature of the QGP, allowing for the study of the QGP in a regime where the QCD coupling constant is small. This facilitates perturbative calculations and theoretical descriptions of the QGP state.
 - The enhanced temperature provides access to higher energy scales and allows for the study of rare processes, such as the production of high-mass resonances and heavy flavor particles, which can provide information about the properties of the QGP.
- QGP phase diagram study in more extreme conditions:
 - By increasing the collision energy, one can explore different regions of the QGP phase diagram, including the search for a possible critical point or the study of the transition from the QGP to hadronic matter.
 - The higher energy allows for measurements of rare phenomena and the investigation of more exotic signatures, such as the search for deconfined quark matter or the formation of exotic states of matter.

Statistics of our analysis

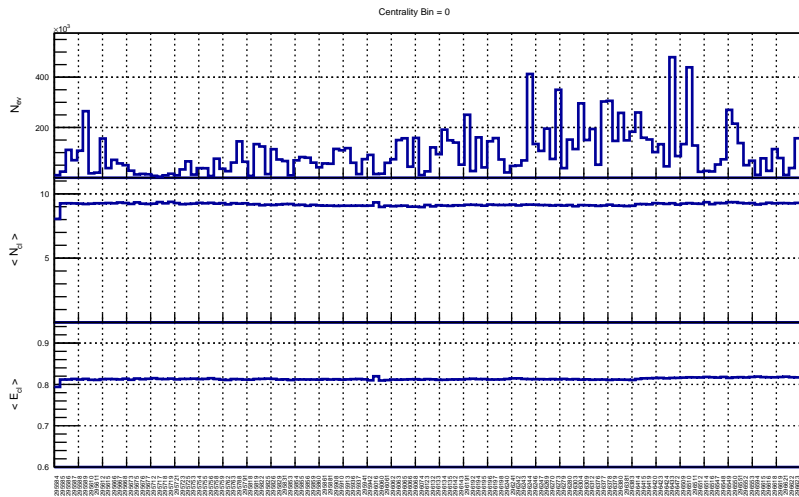
Centrality bin wise event statistics for run period LHC18r and LHC18q

Centrality bin number	Collision centrality	LHC18r	LHC18q
0	0-20%	8.228×10^6	12.97×10^6
1	20-40%	8.268×10^6	13.03×10^6
2	40-60%	8.266×10^6	13.04×10^6
3	60-80%	8.266×10^6	13.04×10^6
4	80-100%	8.206×10^6	12.89×10^6
	Total statistics	41.234×10^6	64.970×10^6

Table: Statistics of events for the run period LHC18r and LHC18q

Run period	Range of run numbers	Number of selected runs
LHC18r	296690-297624	58
LHC18q	295581-296623	131

Table: Selected run number range for our analysis



π^0 invariant mass from two photons decay

- $\pi^0 \rightarrow \gamma + \gamma$
- $M_{\gamma\gamma} = \sqrt{2E_{\gamma_1}E_{\gamma_2}(1 - \cos\theta)}$
- For signal photons from same event are selected and for background signal from different events are also selected

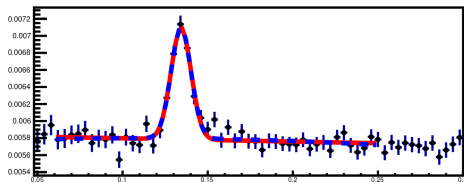
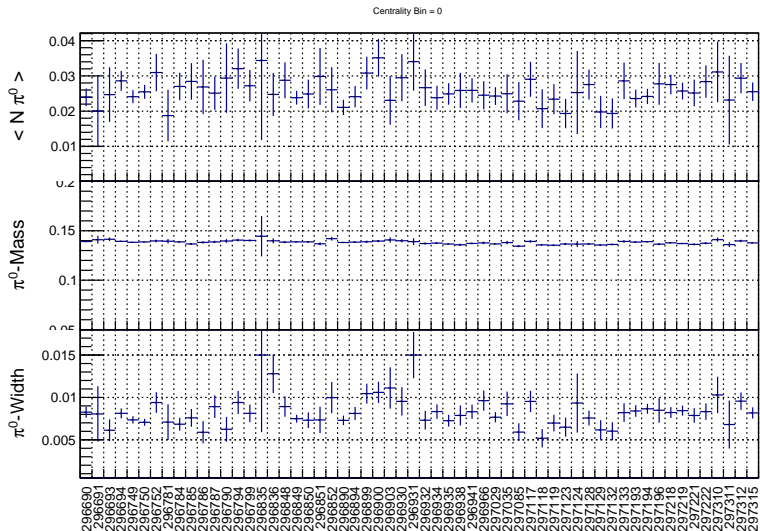
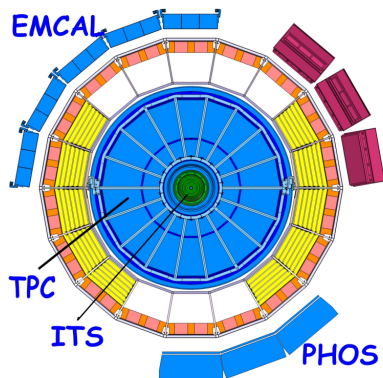


Figure: Gaussian(signal) + second degree polynomial(bkg) fitting

Run-by-run calibration by π^0 invariant mass reconstruction

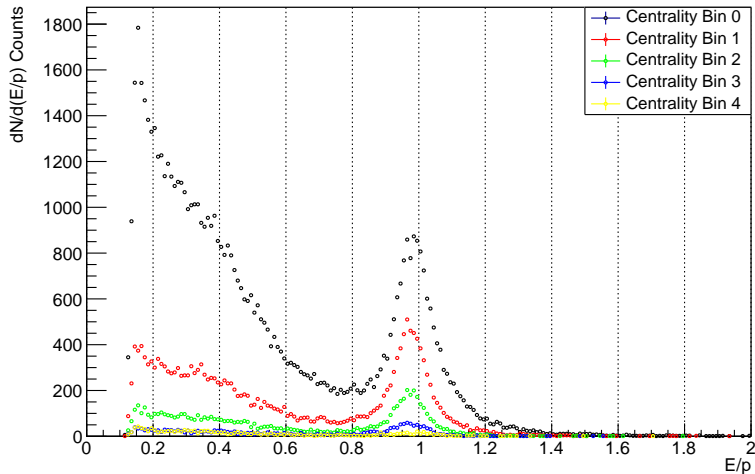


Energy calibration by taking E/p ratio of electrons



- $$E = \sqrt{(p^2 + m_e^2)}$$
- $m_e = 0.0005 \text{ GeV} \ll p (\sim \text{GeV})$
- $E \approx p$ or, $E/p \approx 1$
- 'p' is measured by ITS and TPC using curvature of the trajectory whereas 'E' is measured in PHOS

E/p ratio (electrons and positrons)



Upcoming work plan

- Photon decay background with Monte-Carlo of neutral mesons ($\pi^0, \eta, \omega \dots$)
- Photon sample purity : (Not all clusters are formed by photon)

$$N_{\text{cluster}} = N_{\gamma} + N_{e^{\pm}} + N_{\pi^{\pm}} + N_{K^{\pm}} + N_p + N_{\bar{p}} + N_n + N_{\bar{n}} + N_{K_L^0}$$

$$\text{Purity} = \frac{N_{\gamma}}{N_{\text{cluster}}}$$

- Acceptance and efficiency correction :
 - Not all photons that pass through are detected (dead region, energy threshold, geometric limitations)
 - Trigger efficiency determines how many photons are registered
- Double ratio(R_{γ}) and elliptic flow analysis
- π^0 transverse momentum distribution for different centralities
 - Centrality dependance of photon production

To obtain a physically meaningful results(e.g. yield, elliptic flow etc.) on direct photon production

which is a part of ALICE's effort to reach the following big goals

- To find out whether the QCD transition is of first-order or second order and understanding the formation of QGP and its properties in terms of its temperature, shape, viscosity and equation of state
- Testing the predictions of Field QCD and Lattice QCD
- Understanding quark confinement and parton distribution functions within nucleons

- QCD phase transition and Quark-Gluon Plasma (QGP)
- Advantages of Heavy ion collisions
- Types of direct photons and their measurement
- Previous results demonstrating the presence of direct photons and anisotropic flow
- My analysis of data quality assurance and energy calibration
- Upcoming working plans

THANK YOU FOR LISTENING !